Organic Biradicaloids

International Edition: DOI: 10.1002/anie.201507961
German Edition: DOI: 10.1002/ange.201507961

Cethrene: A Helically Chiral Biradicaloid Isomer of Heptazethrene

*Prince Ravat, Tomáš Šolomek, Michel Rickhaus, Daniel Häussinger, Markus Neuburger, Martin Baumgarten, and Michal Juríček**

Abstract: *We report the synthesis and properties of "cethrene", the only helically chiral isomer of heptazethrene with a biradicaloid singlet ground state. Cethrene gives a well-resolved EPR spectrum at room temperature and its structure was confirmed by 2D NMR and absorption spectroscopies. Our experiments and calculations show that the helical twist affects its electronic properties and decreases the singlet–triplet energy gap when compared to that of planar heptazethrene. Cethrene undergoes an intramolecular cyclization within several hours at room temperature.*

Neutral polycyclic aromatic hydrocarbons that contain one or more unpaired electrons often possess[1,2] an intriguing electronic structure as a result of delocalized spin density. The archetypal example of such a hydrocarbon is phenalenyl[3] (Figure 1), the smallest triangular graphene fragment with an unpaired electron ($S = 1/2$) that determines the propensity of phenalenyl to dimerize[4] via formation of a σ-bond. When this dimerization is suppressed[5] kinetically by the placement of bulky substituents around phenalenyl, it forms a π-dimer through a $2e^-/12$-center bond[6] because of the delocalized spin density. As a result, the π-dimer displays[6c] a large antiferromagnetic exchange interaction in the crystalline state. It has been shown that stable derivatives of phenalenyl capable of such π-dimerization can be employed as molecular conductors,[7] magneto-optical bistable materials,[8] molecular spin batteries,[9] and thermochromic materials.[10]

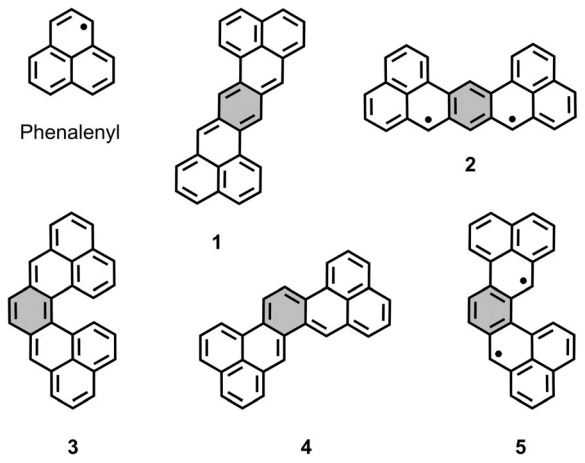

Figure 1. Structural formulae of phenalenyl and heptazethrene (**1**) and its four structural isomers **2**–**5**. In **1**–**5**, two phenalenyl moieties are fused to a central benzene ring (gray) to form either Kekulé (**1**,[1] **3**, and **4**) or non-Kekulé (**2**[1] and **5**) structures.

An extended delocalized multispin system can be formally obtained[11] by fusing two or more phenalenyl units. When two phenalenyl units are fused to a central benzene ring, five possible isomers **1**–**5** can be formed[11a] (Figure 1). Depending on the fusing mode, the two unpaired electrons, one from each phenalenyl, can either couple to provide the Kekulé isomers **1**, **3**, and **4**, which are predicted to have a singlet ground state ($S = 0$), or they remain unpaired to afford the non-Kekulé biradical isomers **2** and **5**, which are predicted to have a triplet ground state ($S = 1$). The Kekulé isomers typically have[12] a low HOMO–LUMO energy gap that endows them with a biradicaloid character, dictating their reactivity and physical properties.

While isomers **3**–**5** remain unknown, derivatives of **1**[1,12] (heptazethrene, "Z-shaped") and **2**[1,13] (heptauthrene, "U-shaped") have been reported, with Kekulé isomer **1** being significantly more stable than the non-Kekulé isomer **2**. Among **1**–**5**, isomer **3** is the only one to have a [5]helicene[14] backbone (highlighted in Scheme 1). Compound **3** therefore possesses properties that arise from its a) unusual electronic structure and b) helical chirality[15] and makes it is possible to investigate how the latter affects the electronic structure. Here, we report the first example (**3a**, Scheme 1) of a chiral neutral polycyclic aromatic hydrocarbon with biradicaloid character, a diphenyl derivative of **3**. We propose the name "cethrene" for the parent hydrocarbon **3** because of its "C-shape" and "chirality". Owing to the sufficiently long lifetime of **3a**, it could be fully characterized by NMR, variable-temperature (VT) EPR, and UV/Vis spectroscopies. The experimental results are supported by theoretical calculations.

The racemic compound **3a** was synthesized in eight steps (Scheme 1) starting from the previously described[16] diphenyl[5]helicene **6** (see the Supporting Information). The selective bromination of **6** at −78 °C gave the key intermediate **7** in 88 % yield. The positions of the two bromine atoms in **7** were confirmed by 2D NMR spectroscopy and single-crystal X-ray diffraction analysis (see the Supporting Information). The Heck reaction of **7** with methyl acrylate gave **8** (69 % yield), which upon the reduction of two double bonds and subsequent demethylation afforded **9** in 85 % yield. The intramolecular Friedel–Crafts acylation of the acyl chloride of

[*] Dr. P. Ravat, Dr. T. Šolomek, Dr. M. Rickhaus, Priv.-Doz.Dr. D. Häussinger, Dr. M. Neuburger, Dr. M. Juríček
Department of Chemistry, University of Basel
St. Johanns-Ring 19, 4056 Basel (Switzerland)
E-mail: michal.juricek@unibas.ch
Prof. M. Baumgarten
Max Planck Institute for Polymer Research
Ackermannweg 10, 55128 Mainz (Germany)

Supporting information and ORCID(s) from the author(s) for this article are available on the WWW under http://dx.doi.org/10.1002/anie.201507961.

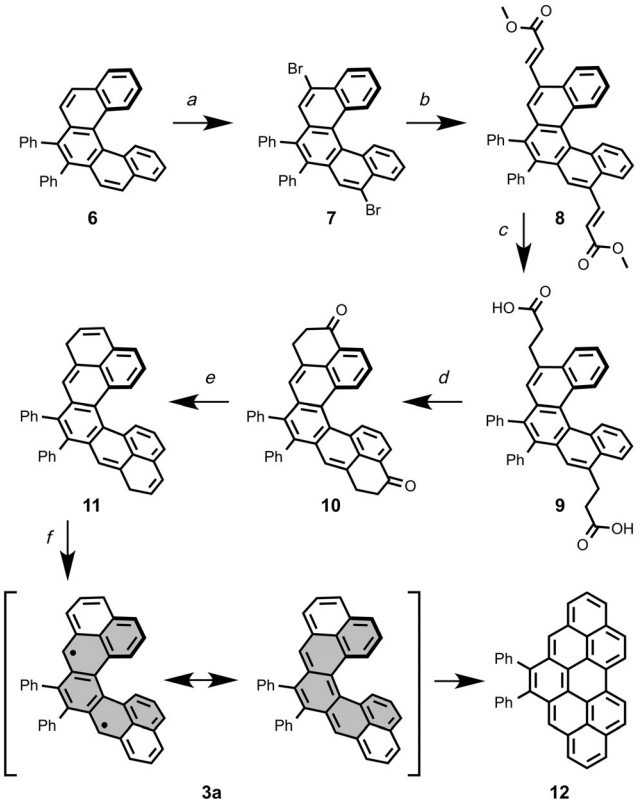

Scheme 1. Synthesis of **3a**: a) Br_2, CH_2Cl_2, −78 to 25 °C, 88%; b) methyl acrylate, $Pd(OAc)_2$, PPh_3, K_2CO_3, Bu_4NBr, DMF, 140 °C, 69%; c) i) H_2, Pd/C, CH_2Cl_2/EtOH, 25 °C, ii) LiI, 2,4,6-collidine, 185 °C, 85%; d) i) $C_2O_2Cl_2$, 65 °C, ii) $AlCl_3$, CH_2Cl_2, −78 to −10 °C, 66%; e) i) $NaBH_4$, CH_2Cl_2/EtOH, 25 °C, ii) *p*-TSA, PhMe, 90 °C, 64%; f) *p*-chloranil. The [5]helicene backbone in **3a** is highlighted in gray.

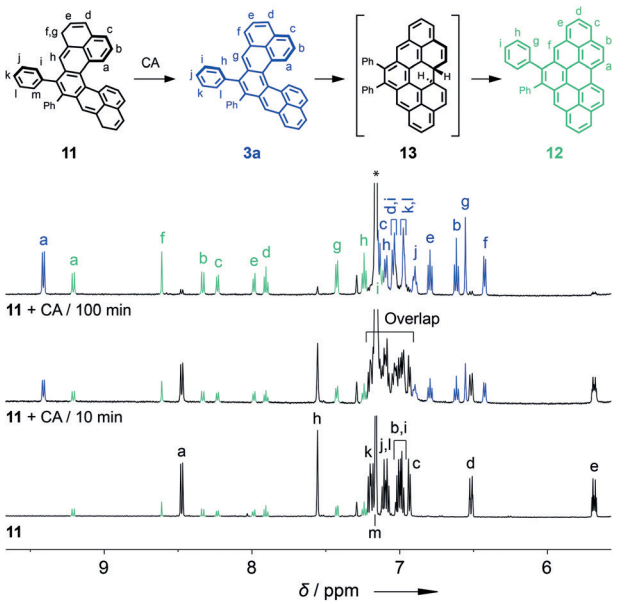

Figure 2. ^{1}H NMR spectra (600 MHz, C_6D_6, 283 K) of **11**, containing < 10% of **12**,[18] before (bottom) and after (middle and top) the addition of *p*-chloranil (CA), with the assignment of proton resonances for **3a**, **11**, and **12**. Asterisk denotes the residual solvent peak.

9 yielded compound **10** in 66% yield, in which all seven six-membered rings are already present. Reduction of **10** and subsequent dehydration afforded racemic **11**, a dihydro precursor of **3a**, in 64% yield. Compound **11** is light-sensitive in air, and its preparation was therefore performed in the dark. Oxidation of **11** with *p*-chloranil (CA) generates the target cethrene **3a**, which could not be isolated as a solid material because it undergoes a relatively fast transformation to the planar hydrocarbon **12** (Figure 2), a process in which two hydrogen atoms are lost. Such formal oxidation was previously observed[17] for a related biphenalenylidene, where a preceding electrocyclization process was proposed. All spectroscopic measurements were therefore performed with a sample of **3a** generated from **11** in situ under argon-saturated conditions.

The progress of the oxidation of **11** with an equivalent amount of CA was studied by ^{1}H NMR spectroscopy (Figures 2 and S1–S13) in CD_2Cl_2 (298 K) and [D_8]toluene or C_6D_6 (283 K) solutions. In all cases, three distinct species, **3a**, **11**, and **12**, were simultaneously present in solution before **11** was consumed. At a certain point, the concentration of **3a** reached its maximum and then **3a** gradually diminished leaving **12** the only species in solution. The reaction ran to completion within 10 min at 298 K in CD_2Cl_2 (Figure S1). In [D_8]toluene and C_6D_6, the proton signals of **3a** were observable even after several hours at 283 K. No other intermediate was observed prior to formation of **12**, which suggests that the decay of the putative **13** must be significantly faster than its formation from **3a**. The 2D HSQC and HMBC NMR experiments allowed us to unambiguously assign all proton and carbon resonances for **3a** and **12** (Figures S12 and S13) to the corresponding atoms providing definitive structural proof for both compounds. The proton H_a shows the most downfield chemical shift for **3a** and **11**, indicating a [5]helicene backbone for both compounds (compare with **6**, Table S1). The observation that the diffusion coefficient of **3a** ($D = 5.79 \times 10^{-10}$ m^{2}s^{-1}) is smaller than that of **12** ($D = 6.59 \times 10^{-10}$ m^{2}s^{-1}) also reflects the expected difference in their shapes (PFGSE NMR, Figure S7).

Owing to the distinctive UV/Vis spectra (Figure 3) of **11** ($\lambda_{max} = 312$ nm) and **12** ($\lambda_{max} = 485$ nm) in toluene, absorption spectroscopy was used used to monitor (Figure S14) the reaction progress. Immediately after the addition of CA to the solution of **11**, a new broad absorption band appeared at $\lambda_{max} = 665$ nm. Its intensity increased and the band gradually disappeared within 5 h at 298 K in accord with the NMR observations. The calculations (Table S2) for **3a** predicted a S_0–S_1 transition at $\lambda_{calc} = 708$ nm. The observed low-energy absorption band can therefore be attributed to **3a**, in agreement with the absorption[17] of biphenalenylidene. The absorption spectrum of **1** reported[1] by Clar showed an absorption band at $\lambda_{max} = 586$ nm ($\lambda_{calc} = 587$ nm). The bathochromic shift observed for **3a** indicates that its HOMO–LUMO gap is smaller than that of the planar **1** ($\Delta E_{HOMO-LUMO} = 1.79$ and 1.68 eV for **1** and **3**, respectively; Table S2).

Freshly generated **3a** in argon-saturated toluene ($c \approx 10^{-4}$ M) gave an EPR signal for triplet **3a** at 290 K with a *g*-value of 2.0024 (Figure 4). The proton hyperfine coupling

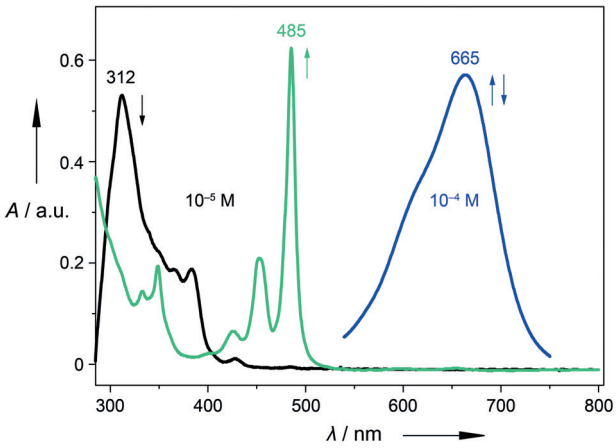

Figure 3. UV/Vis spectra (toluene, 298 K) of a solution of **11** before (black, $c \approx 10^{-5}$ M) and after (blue, $c \approx 10^{-4}$ M, after 45 min; green, $c \approx 10^{-5}$ M, after 24 h) the addition of *p*-chloranil. The peaks at $\lambda_{max} = 665$ nm (blue) and $\lambda_{max} = 485$ nm (green) belong to **3a** and **12**, respectively.

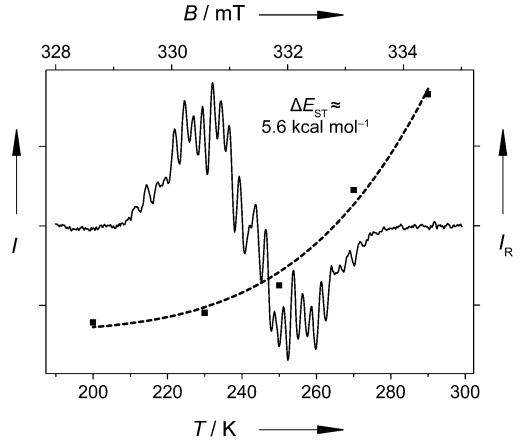

Figure 4. EPR spectrum (solid line, top and right axes) recorded for a solution of **11** in toluene after the addition of *p*-chloranil at 290 K. The Bleaney–Bowers fit[19] (dashed line, bottom and left axes) to the variable-temperature EPR data (black squares, Figure S15) gave a S–T gap value of roughly 5.6 kcal mol^{-1}. I and I_R are the integrated and relative intensity, respectively.

constants (a_N) could not be determined from our experimental data due to the large number of non-equivalent protons. The EPR spectrum simulated using the a_N values (Figure S16 and Table S3) obtained from a DFT calculation is in good qualitative agreement with experiment. The a_N values indicate that the unpaired electrons are largely delocalized (Figure 5). The signal intensity decreased at lower temperatures (Figure S15) in accord with singlet being the ground state, and the Bleaney–Bowers fit[19] to our data provided the singlet–triplet (S–T) energy gap $\Delta E_{ST} \approx 5.6$ kcal mol^{-1}, which is in excellent agreement with the calculated value of 5.9 kcal mol^{-1} (Table 1). This gap is markedly lower than that (8.9 kcal mol^{-1}) calculated for planar **1**. The smaller S–T gap can be attributed to the helical twist in **3**, as further supported by the calculated $\Delta E_{ST} = 8.0$ kcal mol^{-1} for hypothetical planar $\mathbf{3_{pl}}$ (Table S4). The HOMO is antisymmetric, while the LUMO is symmetric with respect to the rotation around the C_2 axis of **3**.[20] When $\mathbf{3_{pl}}$ is twisted, an antibonding and bonding interaction (Figure 5) within the HOMO and the LUMO, respectively, appear between the carbon atoms bearing protons H_a. In triplet **3**, the HOMO and the LUMO are occupied by one electron each, while the two electrons are predominantly paired in the HOMO of singlet **3**. Consequently, the triplet suffers less than the singlet from the antibonding interaction in the HOMO and profits from the bonding interaction in the LUMO, resulting in its stabilization and decrease of the S–T gap of **3** compared with that of $\mathbf{3_{pl}}$ or **1**.

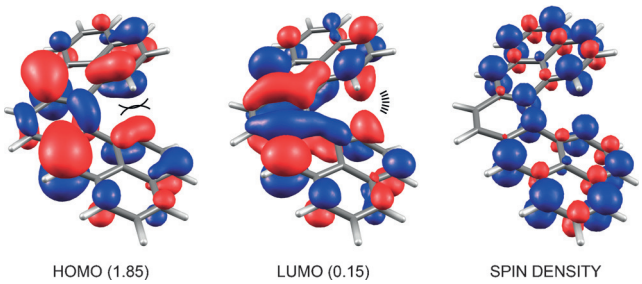

Figure 5. HOMO (left) and LUMO (middle) of **3** obtained from CAS-(12,12) calculations (occupation numbers shown) and the spin-density distribution of triplet **3** (right) obtained from U-B3LYP calculations.

Table 1: Calculated[a] S–T energy gap ($\Delta E_{ST} = E_T - E_S$) of **3** and the energy difference ($\Delta E_{BS/RS} = E_{RS} - E_{BS}$) of the spin-unrestricted broken-symmetry (BS) and restricted (RS) singlet DFT wavefunctions.

ΔE [kcal mol^{-1}]	B3LYP	CAM-B3LYP	BMK	M06-2X
ΔE_{ST}[b,c]	5.9	2.2 (6.6[c,d])	5.8	7.9
$\Delta E_{BS/RS}$	0.0	2.7	−0.1	N/A[e]

[a] Computed with the cc-pVTZ basis set on the 6-31G(d) geometries. [b] Restricted DFT was used to model the singlet states. [c] ZPVE corrections are included. [d] Spin-unrestricted broken-symmetry singlet wavefunction was used. [e] Not available (see the Supporting Information).

The electronic structure of **3** was studied (Table 1) computationally in more detail. We found that, among the functionals used, the energy difference of the spin-unrestricted broken-symmetry (BS) and restricted (RS) singlet wavefunction is negligible. CAM-B3LYP comes as an exception, and the use of BS wavefunction was necessary to obtain a reliable value for the S–T gap. The frontier MO occupation numbers (HOMO: 1.85, LUMO: 0.15) obtained from a CAS-(12,12) calculation (see the Supporting Information), which treats the static electron correlation correctly, shows a modest biradicaloid character of **3**. The shape of the HOMO and the LUMO (Figure 5) suggests that the electron density in singlet **3** is localized on the central ring to a greater extent than on the rings of the phenalenyl subunits, which is in good agreement with both the bond lengths (Table S5) and NICS profiles (Figure S20) obtained from DFT. The latter confirms clearly that **3** is best represented by the quinoidal resonance structure (Scheme 1).

To confirm that **3a** is chiral, we separated (HPLC on a chiral stationary phase, Figure S17) the enantiomers of **11**, which display mirror-image CD responses (Figure S18) in EtOH/MeOH (1:1), and assigned the absolute configuration of each enantiomer with the help of TD-DFT calculations. The racemization barrier was determined (Figure S19) to be (25.2 ± 0.024) kcal mol^{-1} at 298 K, a value which is slightly higher than that (24.1 kcal mol^{-1} at 298 K)[14] of [5]helicene. Although the CD spectra for **3a** could not be obtained because of the low signal-to-noise ratio, the racemization time of several days of **11** indicates that **3a** is stable against racemization within its lifetime at 298 K.

In summary, we have synthesized a diphenyl derivative of cethrene, the first chiral neutral polycyclic aromatic hydrocarbon with biradicaloid character. The helical twist in cethrene results in a significant decrease of the S–T gap relative to that of heptazethrene. By placing suitable substituents at the positions bearing H_a protons, one could prevent the formation of **12** and study the electrocyclization of **3**. Understanding this process could enable the isolation of **3** or its derivative as a solid material.

Acknowledgements

We thank Prof. Dr. Marcel Mayor for generously hosting our group at the University of Basel and his invaluable support of our research, and gratefully acknowledge the computational facilities provided by the University of Fribourg. The Swiss National Science Foundation (SNF, M.J./PZ00P2_148043 and D.H./200021_130263), the Novartis University of Basel Excellence Scholarship for Life Sciences (P.R. and M.J.), the Experientia Foundation (T.Š.), and the German Science Foundation (DFG, M.B./SFB/TR49) are gratefully acknowledged for their financial support.

Keywords: biradicaloids · cethrene · chirality · helical structures · zethrene

How to cite: *Angew. Chem. Int. Ed.* **2016**, *55*, 1183–1186
Angew. Chem. **2016**, *128*, 1198–1202

[1] E. Clar, I. A. Macpherson, *Tetrahedron* **1962**, *18*, 1411–1416.
[2] *Carbon Based Magnetism* (Eds.: T. Makarova, F. Palacio), Elsevier, Amsterdam, **2006**.
[3] a) T. Kubo, *Chem. Rec.* **2015**, *15*, 218–232; b) Y. Morita, S. Suzuki, K. Sato, T. Takui, *Nat. Chem.* **2011**, *3*, 197–204; c) Y. Morita, S. Nishida in *Stable Radicals: Fundamentals and Applied Aspects of Odd-Electron Compounds* (Ed.: R. G. Hicks), Wiley, Chichester, **2010**, pp. 81–145.
[4] a) D. H. Reid, *Q. Rev. Chem. Soc.* **1965**, *19*, 274–302; b) P. B. Sogo, M. Nakazaki, M. Calvin, *J. Chem. Phys.* **1957**, *26*, 1343–1345.
[5] K. Goto, T. Kubo, K. Yamamoto, K. Nakasuji, K. Sato, D. Shiomi, T. Takui, M. Kubota, T. Kobayashi, K. Yakusi, J. Y. Ouyang, *J. Am. Chem. Soc.* **1999**, *121*, 1619–1620.
[6] a) Z.-H. Cui, H. Lischka, H. Z. Beneberu, M. Kertesz, *J. Am. Chem. Soc.* **2014**, *136*, 5539–5542; b) Z. Mou, K. Uchida, T. Kubo, M. Kertesz, *J. Am. Chem. Soc.* **2014**, *136*, 18009–18022; c) Y. Takano, T. Taniguchi, H. Isobe, T. Kubo, Y. Morita, K. Yamamoto, K. Nakasuji, T. Takui, K. Yamaguchi, *J. Am. Chem. Soc.* **2002**, *124*, 11122–11130.
[7] a) S. K. Mandal, S. Samanta, M. E. Itkis, D. W. Jensen, R. W. Reed, R. T. Oakley, F. S. Tham, B. Donnadieu, R. C. Haddon, *J. Am. Chem. Soc.* **2006**, *128*, 1982–1994; b) S. K. Pal, M. E. Itkis, F. S. Tham, R. W. Reed, R. T. Oakley, R. C. Haddon, *Science* **2005**, *309*, 281–284; c) X. Chi, M. E. Itkis, K. Kirschbaum, A. A. Pinkerton, R. T. Oakley, A. W. Cordes, R. C. Haddon, *J. Am. Chem. Soc.* **2001**, *123*, 4041–4048.
[8] a) R. G. Hicks, *Nat. Chem.* **2011**, *3*, 189–191; b) M. E. Itkis, X. Chi, A. W. Cordes, R. C. Haddon, *Science* **2002**, *296*, 1443–1445.
[9] Y. Morita, S. Nishida, T. Murata, M. Moriguchi, A. Ueda, M. Satoh, K. Arifuku, K. Sato, T. Takui, *Nat. Mater.* **2011**, *10*, 947–951.
[10] Y. Morita, S. Suzuki, K. Fukui, S. Nakazawa, H. Kitagawa, H. Kishida, H. Okamoto, A. Naito, A. Sekine, Y. Ohashi, M. Shiro, K. Sasaki, D. Shiomi, K. Sato, T. Takui, K. Nakasuji, *Nat. Mater.* **2008**, *7*, 48–51.
[11] a) Z. Sun, Z. Zeng, J. Wu, *Acc. Chem. Res.* **2014**, *47*, 2582–2591; b) A. Shimizu, T. Kubo, M. Uruichi, K. Yakushi, M. Nakano, D. Shiomi, K. Sato, T. Takui, Y. Hirao, K. Matsumoto, H. Kurata, Y. Morita, K. Nakasuji, *J. Am. Chem. Soc.* **2010**, *132*, 14421–14428; c) T. Kubo, A. Shimizu, M. Uruichi, K. Yakushi, M. Nakano, D. Shiomi, K. Sato, T. Takui, Y. Morita, K. Nakasuji, *Org. Lett.* **2007**, *9*, 81–84; d) T. Kubo, A. Shimizu, M. Sakamoto, M. Uruichi, K. Yakushi, M. Nakano, D. Shiomi, K. Sato, T. Takui, Y. Morita, K. Nakasuji, *Angew. Chem. Int. Ed.* **2005**, *44*, 6564–6568; *Angew. Chem.* **2005**, *117*, 6722–6726.
[12] a) Z. Sun, S. Lee, K. H. Park, X. Zhu, W. Zhang, B. Zheng, P. Hu, Z. Zeng, S. Das, Y. Li, C. Chi, R.-W. Li, K.-W. Huang, J. Ding, D. Kim, J. Wu, *J. Am. Chem. Soc.* **2013**, *135*, 18229–18236; b) Y. Li, W.-K. Heng, B. S. Lee, N. Aratani, J. L. Zafra, N. Bao, R. Lee, Y. M. Sung, Z. Sun, K.-W. Huang, R. D. Webster, J. T. López Navarrete, D. Kim, A. Osuka, J. Casado, J. Ding, J. Wu, *J. Am. Chem. Soc.* **2012**, *134*, 14913–14922; c) Z. Sun, K.-W. Huang, J. Wu, *J. Am. Chem. Soc.* **2011**, *133*, 11896–11899.
[13] Y. Li, K.-W. Huang, Z. Sun, R. D. Webster, Z. Zeng, W. Zeng, C. Chi, K. Furukawa, J. Wu, *Chem. Sci.* **2014**, *5*, 1908–1914.
[14] C. Goedicke, H. Stegemeyer, *Tetrahedron Lett.* **1970**, *11*, 937–940.
[15] A. Ueda, H. Wasa, S. Suzuki, K. Okada, K. Sato, T. Takui, Y. Morita, *Angew. Chem. Int. Ed.* **2012**, *51*, 6691–6695; *Angew. Chem.* **2012**, *124*, 6795–6799.
[16] a) S. Goretta, C. Tasciotti, S. Mathieu, M. Smet, W. Maes, Y. M. Chabre, W. Dehaen, R. Giasson, J.-M. Raimundo, C. R. Henry, C. Barth, M. Gingras, *Org. Lett.* **2009**, *11*, 3846–3849; b) M. Shimizu, I. Nagao, Y. Tomioka, T. Hiyama, *Angew. Chem. Int. Ed.* **2008**, *47*, 8096–8099; *Angew. Chem.* **2008**, *120*, 8216–8219.
[17] S. Pogodin, I. Agranat, *J. Am. Chem. Soc.* **2003**, *125*, 12829–12835.
[18] Compound **11** typically contained small amounts (< 10%) of compound **12**, because light and air could not be completely avoided during the purification.
[19] a) B. Bleaney, K. D. Bowers, *Proc. R. Soc. London Ser. A* **1952**, *214*, 451–465; b) P. Ravat, M. Baumgarten, *Phys. Chem. Chem. Phys.* **2015**, *17*, 983–991.
[20] Helical and planar **3** belong to C_2 and C_{2v} point groups of symmetry, respectively.

Received: August 25, 2015
Published online: November 23, 2015

